CERN-EP/98-41
MPI-K H V5 1998

6 March 1998

Charge Asymmetries for D, D_s and Λ_c Production in Σ^- - Nucleus Interactions at 340 GeV/c

The WA89 Collaboration

M.I. Adamovich[8], Yu.A. Alexandrov[8], D. Barberis[3], M. Beck[5], C. Bérat[4], W. Beusch[2], M. Boss[6], S. Brons[5,a], W. Brückner[5], M. Buénerd[4], C. Busch[6], C. Büscher[5], F. Charignon[4], J. Chauvin[4], E.A. Chudakov[6,b], U. Dersch[5], F. Dropmann[5], J. Engelfried[6,c], F. Faller[6,d], A. Fournier[4], S.G. Gerassimov[5,8], M. Godbersen[5], P. Grafström[2], Th. Haller[5], M. Heidrich[5], E. Hubbard[5], R.B. Hurst[3], K. Königsmann[5,e], I. Konorov[5,8], N. Keller[6], K. Martens[6,f], Ph. Martin[4], S. Masciocchi[5,g], R. Michaels[5,h], U. Müller[7], H. Neeb[5], D. Newbold[1], C. Newsom[i], S. Paul[5,j], J. Pochodzalla[5], I. Potashnikova[5], B. Povh[5], R. Ransome[k], Z. Ren[5], M. Rey-Campagnolle[4,l], G. Rosner[7], L. Rossi[3], H. Rudolph[7], C. Scheel[m], L. Schmitt[7,j], H.-W. Siebert[6], A. Simon[6,e], V.J. Smith[1,n], O. Thilmann[6], A. Trombini[5], E. Vesin[4], B. Volkemer[7], K. Vorwalter[5], Th. Walcher[7], G. Wälder[6], R. Werding[5], E. Wittmann[5], and M.V. Zavertyaev[8]

[1] *University of Bristol, Bristol BS8 1TL, United Kingdom.*
[2] *CERN, CH-1211 Genève 23, Switzerland.*
[3] *Dipartimento di Fisica and I.N.F.N., Sezione di Genova, I-16146 Genova, Italy.*
[4] *ISN, CNRS/IN2P3-UJF, 53 Avenue des Martyrs, F-38026 Grenoble Cedex, France.*
[5] *Max-Planck-Institut für Kernphysik Heidelberg, D-69029 Heidelberg, Germany.*
[6] *Physikalisches Institut, Universität Heidelberg, D-69120 Heidelberg, Germany.*[o]
[7] *Institut für Kernphysik, Universität Mainz, D-55099 Mainz, Germany.*[o]
[8] *Moscow Lebedev Physics Institute, RU-117924 Moscow, Russia.*

Abstract

CERN experiment WA89 has studied charmed particles produced by a Σ^- beam at 340GeV/c on nuclear targets. Production of particles which have light quarks in common with the beam is compared to production of those which do not. Considerable production asymmetries between D^- and D^+, D_s^- and D_s^+ and Λ_c and $\overline{\Lambda}_c$ are observed. The results are compared with pion beam data and with theoretical calculations.

(Submitted to European Physical Journal C)

[a] *Now at TRIUMF, Vancouver, B.C., Canada V6T 2A3.*
[b] *On leave of absence from Moscow State University, 119889 Moscow, Russia.*
[c] *Now at FNAL, PO Box 500, Batavia, IL 60510, USA.*
[d] *Now at Fraunhofer Institut für Solarenergiesysteme, D-79100 Freiburg, Germany.*
[e] *Now at Fakultät für Physik, Universität Freiburg, Germany.*
[f] *Now at Institute for Cosmic Ray Research, University of Tokyo,Japan.*
[g] *Now at Max-Planck-Institut für Physik, München, Germany*
[h] Now at Thomas Jefferson Lab, Newport News, VA 23606, USA.
[i] *University of Iowa, Iowa City, IA 52242, USA.*
[j] *Now at Technische Universitaät München, Garching, Germany*
[k] *Rutgers University, Piscataway, NJ 08854, USA.*
[l] *permanent address: CERN, CH-1211 Genève 23, Switzerland*
[m] *NIKHEF,1009 DB Amsterdam, The Netherlands.*
[n] *supported by the UK PPARC.*
[o] *supported by the Bundesministerium für Bildung, Wissenschaft, Forschung und Technologie, Germany, under contract numbers 05 5HD15I, 06 HD524I and 06 MZ5265.*

1 Introduction

In hadronic interactions, typically, the forward production of particles which have valence quarks/antiquarks in common with the beam (leading particles) is enhanced over those which do not (non–leading particles). This "leading particle effect" is strongly pronounced and well known in the light quark sector, for example in the production of strange particles (see for example [1] and the references therein). Hadroproduction of charmed particles is usually described by splitting it into a "hard" process of $c\overline{c}$ production and a "soft" process of hadronisation of $c/\overline{c}$ quarks to real hadrons. The production of $c\overline{c}$ pairs has been described by next-to-leading order (NLO) PQCD calculations [2, 3] which do not predict significant asymmetries between the c and $\overline{c}$ produced [6]. For the hadronisation, however, only phenomenological models exist. Since no charm/anti–charm production asymmetries have been observed in e^+e^- interactions, while large asymmetries have been observed in charm hadroproduction, the observed asymmetries can be accounted for by recombination of charm quarks/anti–quarks with the valence quarks from the beam particle. In this picture the leading particle effect would be expected to increase at larger x_F, which indeed has been observed (see later). Since the differential cross–sections of charmed particles are observed to drop sharply with increasing x_F, no considerable asymmetry between cross–sections of leading and non–leading particles integrated for $x_F{>}0$ is expected.

At present, there are high statistics data on D^- and D^+ production in π^- beams [4–7], which show a considerable enhancement of leading D^- over non-leading D^+ in the kinematic range of $x_F{>}0.3$. The asymmetry parameter A:

$$A(x_F) = \frac{d^3\sigma_L/dp^3 - d^3\sigma_{NL}/dp^3}{d^3\sigma_L/dp^3 + d^3\sigma_{NL}/dp^3} \tag{1}$$

constructed using differential cross–sections of the leading and non–leading particles, rises with x_F and reaches values of A$\approx$ 0.5 at x_F=0.6 . No asymmetry between D_s^- and D_s^+ or Λ_c and $\overline{\Lambda}_c$ production by pion beams is observed [7–9]. In contrast to the high statistics of the pion beam data (up to 75000 reconstructed D^- plus D^+ in [6]) only limited data exist on charmed particle production by other hadron beams. The results obtained in pp–interactions at 400 GeV/c by the the LEBC-EHS experiment [10] which has observed about 50 D^- plus D^+ candidates indicated a "harder" x_F spectrum for the non–leading D^+ than for the leading D^-. No significant difference in the number of observed Λ_c and $\overline{\Lambda}_c$ was found in a sample of 7 candidates. Due to the low statistics no distinction between leading and non–leading particles produced by 200 GeV/c protons in the ACCMOR experiment [11] was done. In a proton beam of 250 GeV/c of experiment E769 [12] an asymmetry integrated for $x_F{>}0$ of $A(D^{\pm})$=0.18$\pm$0.05 has been observed, comparable to the asymmetry measured in the pion beam of the same experiment [5] of $A(D^{\pm})$=0.18$\pm$0.06. [1] The same experiment observed a large asymmetry $A(\Lambda_c){>}$ 0.6 with a limited sample of about 35 Λ_c. These results indicate a leading particle effect in charm production by protons, in contrast to the older results from [10]. In kaon beams it is of a particular interest to compare the production of D_s^+ and D_s^-. The only asymmetry result comes from the same experiment [12] which measured $A(D_s)$ integrated for $x_F{>}0$ and reported a value of 0.25$\pm$0.11.

It is therefore interesting to look for the leading particle effect in baryon beams as well as in strange beams. The most recent hyperon beam experiment, WA89 at CERN, used a Σ^- beam which offers the opportunity to look for leading particle effects with charmed–strange particles and with charmed baryons. In this paper the results on production of D^- versus D^+, D_s^- versus D_s^+ and

[1] It is not quite clear from the paper [12] why the errors for these two asymmetries happen to be the same, while one may infer from the paper that the statistics obtained in the pion beam was about 4 times higher than in the proton beam.

Λ_c versus $\overline{\Lambda}_c$ are presented. The first particle in each pair is leading in a Σ^- beam while the second particle is not. Neutral D^0 and $\overline{D}^0$ are not considered since the direct production is non–leading for both particles while a considerable fraction of them can come from decays of charged higher states.

2 Experimental Setup

Experiment WA89 was performed using the charged hyperon beam [13] of the CERN SPS. The setup was based on a magnetic spectrometer which detected decays of charmed particles produced at x_F>0.1. Hyperons were produced by 450 GeV/c protons impinging on a 40 cm long beryllium target with a diameter of 0.2 cm. A magnetic channel consisting of 3 magnets selected negative particles with a mean momentum of 345 GeV/c, a momentum spread of $\sigma(p)/p = 9\%$, and an angle to the proton beam smaller than 0.5 mrad. After travelling a distance of 16 m the secondary beam hit the charm production target which consisted of one 4 mm thick copper plate followed by three 2 mm thick carbon plates made of diamond powder with a density of 3.3 g/cm^3. The target plates were spaced by 2 cm. At the target the beam had a width of 3 cm and a height of 1.7 cm. Its angular dispersion was 0.6 mrad in the horizontal plane and 1.0 mrad in the vertical plane. An incoming intensity of $4.0 \cdot 10^{10}$ protons per 2.1 second spill yielded about $1.8 \cdot 10^5$ Σ^- hyperons and $4.5 \cdot 10^5$ π^- at the charm production target. A transition radiation detector (TRD) [14] was used to discriminate online between π^- and hyperons.

Fig. 1 shows the experimental setup. The incoming beam particles and the secondary particles were detected by a set of silicon micro-strip planes with 25 and 50μm pitch. The micro-strip detectors measured the horizontal, vertical and $\pm 45^o$ projections.

Positioning the charm production target about 14 m upstream of the centre of the Ω-spectrometer provided a 10 m long decay volume for short living strange particles. The charged products of these decays along with the particles coming directly from the target were detected by 40 planes of drift chambers with a spatial resolution of about 300 μm. Special MWPC chambers (20 planes with 1mm wire spacing) were used in the central region of high particle fluxes. In order to improve the track bridging between the target region and the decay region three sets of 4 MWPCs each with a pitch of 1 mm were installed about 2 m downstream of the charm production target. The particle momenta were measured by the Ω-spectrometer [15] consisting of a super-conducting magnet with a field integral of 7.5 Tm and a tracking detector consisting of 45 MWPC planes inside the field and 12 drift chamber planes at the exit of the magnet. The momentum resolution was $\sigma(p)/p^2 \approx 10^{-4}$ (GeV/c)$^{-1}$.

Charged particles were identified using a ring imaging Cherenkov (RICH) detector [16]. This had a threshold of $\gamma = 42$ and provided K/π separation from about 8 to 90 GeV/c with about 90% efficiency and a pion rejection of a factor 10 or more. The geometrical aperture of the RICH was nearly 100% for particles with momenta >15 GeV/c. Downstream of the RICH a lead glass electromagnetic calorimeter was positioned for photon and electron detection [17]. This calorimeter was in turn followed by a hadron calorimeter [18].

The trigger was relatively open. It selected about 25% of all interactions using the multiplicity measured in scintillator hodoscopes and proportional chambers and using correlations of hits in these detectors to select particles with high momenta. At least two charged particles at the exit of the magnet were required. The results shown in the present paper are based on the analysis of about 300 million events recorded in 1993 and 1994.

3 Data Analysis

The goal was to compare leading and non–leading charmed particles which are charge–conjugate: D^- and D^+, D_s^- and D_s^+ and Λ_c and $\overline{\Lambda}_c$. We looked for 3-body decays: $D^- \rightarrow K^+\pi^-\pi^-$, $D_s^- \rightarrow K^+K^-\pi^-$, $\Lambda_c \rightarrow K^-p\pi^+$, and the charge–conjugate states. The acceptance of the setup is nearly independent of the particle charge (see 3.2) and therefore the systematic errors of a comparison of conjugate decay modes should be minimal. The key elements of the charm identification are geometrical reconstruction of events with two or more vertices and identification of kaons with the RICH.

3.1 Event reconstruction

The reconstruction started with a fast rejection of events which had no valid interaction in the target by cutting on the track multiplicities before and after the target. Additionally, secondary interactions were suppressed by rejecting large differences in multiplicity between the target region and the spectrometer. Charged particle trajectories were reconstructed in the Ω spectrometer (for a detailed description see [19]), in the decay region and vertex detector, then all track segments were bridged together if possible. Particle identification of protons and kaons was performed with the RICH.

The charm search was based on a "candidate–driven approach". All relevant combinations of 3 tracks were considered and the coordinates of their origin – the potential secondary vertex – were reconstructed. The rest of the tracks, including the beam track if it was found, were used to form the interaction point – the primary vertex – in the target. These tracks were subjected to a filter in order to remove tracks coming from decays of associated charmed particles, misreconstructed tracks and other tracks which did not originate in the interaction point. Some of such tracks passed through the filter causing systematic distortions of the primary vertex. The most powerful charm selection criterion was rejection of events with a small separation between the secondary and primary vertices. The typical resolution on the longitudinal distance between these vertices was about 0.5 mm while the typical mean decay lengths of the charmed particles we looked for were 3–15 mm. One set of selection criteria was used for all charm decays considered, including the following cuts:

- a longitudinal separation between the vertices of >8–9σ, depending on the particle type; the secondary vertex to be outside of the target material by $> 1 - 3\sigma$;
- impact parameters of the tracks from the secondary vertex to the primary vertex of $>2\sigma$;
- an impact parameter of the reconstructed track of the charm particle candidate to the primary vertex of $<4\sigma$;
- "soft" RICH identification of kaons and protons, mainly rejecting clearly identified pions.

The values of the cuts were identical for the charge–conjugate modes, while the above cuts on vertex separation were slightly different for different particles because of the different decay geometries.

The resulting invariant mass spectra for the six decays modes are presented in Fig. 2. Clear signals are observed for D^-, D^+, D_s^- and Λ_c, while no significant mass peaks are observed for D_s^+ and $\overline{\Lambda}_c$. Small signals of about 5-10 events for the two latter particles are observed with harder cuts. Such harder cuts, however, reduce the signals for D_s^- and Λ_c and increase the statistical error on the estimate of the production asymmetry. The numbers of observed signal and background

events as well as the deviations of the signals from the PDG [20] masses are shown in Table 1. There are no multiple entries from one event to the signal regions. Possible mutual reflections of the mass peaks have been studied. Due to a good kaon and proton identification these reflections are not strong. The contamination of the D_s^- signal with D^- is estimated to be below 8 events, and the contamination of the Λ_c signal with D^+ is estimated to be below 3 events.

3.2 Acceptance Corrections

If the acceptance of the experiment is truly charge independent one could measure the x_F dependence of the asymmetry between two charge–conjugate states without correcting for the acceptance, provided that the bins in x_F were small enough. In WA89 the acceptance was nearly symmetric, however the efficiency of the trigger and the RICH introduced a slight charge asymmetry. Therefore we used the full calculation of charm reconstruction efficiencies in order to correct the x_F spectra observed. Charm events were simulated by an inclusive event generator that generated the charm particle considered, according to the measured kinematic distributions together with an associated anti–charm particle. The latter was produced with the same kinematic distributions as the first particle, taking into account an azimuthal angular correlation with the first particle, measured in a pion beam [21]. For the associated particles a mixture of about 25% of charged D-mesons, 50% of neutral D-mesons, and 25% of Λ_c was taken, in accordance with average yields of charmed particles measured in various experiments. The remaining multiplicity of the interaction was generated using the FRITIOF Monte Carlo for hadron–nucleus interactions [22]. The particles were tracked through the detector by a detector simulation program based on the GEANT package [23]. The response functions of the different detector components and the trigger were simulated according to the measured efficiencies. The trigger logic was simulated as well. The simulated events were then analysed using the regular track reconstruction and charm reconstruction procedure, and the acceptances of the experiment to the decay modes studied were evaluated applying the whole set of selection criteria used for the data. The number of reconstructed simulated charm events was at least one order of magnitude higher than the size of the charm signals observed in the data.

The acceptance of the experiment does not depend strongly on the transverse momentum of the charmed particles up to p_T=2 GeV/c. Most of the charm events observed had p_T<1.5 GeV/c. Therefore only the x_F dependence of the acceptance was considered. These dependences for D^- and D^+ averaged for the 1993 and 1994 runs of data–taking are shown in Fig. 3. The acceptances drop sharply at x_F<0.2 and are very low at x_F<0.1. A loss of efficiency at high x_F is caused by the charm reconstruction technique which required the reconstruction of the primary vertex built of leftover tracks. For high x_F there are fewer leftover particles with momentum high enough to be reconstructed. The efficiencies for the charge–conjugate modes differ by about 10%. The calculated charm reconstruction efficiency for the 1994 run was about 40% higher than for 1993 (see Table 2), due to a better vertex detector and the choice of charm selection cuts. However for this analysis only the relative efficiencies for charge conjugated modes within one run are important.

3.3 Production Asymmetries

Comparison of the observed raw number of events shows a considerable enhancement of the leading over non–leading particles in the useful kinematic range of x_F>0.1, taking into account that the acceptances for them are close. For a quantitative estimate the data were split in bins of x_F separately for the 1993 and 1994 data. The value of x_F was calculated using a fixed beam momentum of 340 GeV/c. Since the number of events observed in a bin was low, in particular at high x_F, we calculated the values of the asymmetry and the errors using the maximum likelihood method.

For a given x_F bin we took the number of events N – in the signal mass window of ± 20 MeV/c^2 and B – in the sidebands of -140 to -20 MeV/c^2 and 20-140 MeV/c^2 with respect to the table mass of the particle. The numbers N and B along with the calculated efficiencies $\mathcal{E}$ and its errors are summarised in Table 2. Since the background in the mass spectra is well described by a linear distribution, we estimate the expected number of background events in the signal window as $\alpha \cdot B$, where $\alpha = 1/6$. The parameters used were the expectation values for the background in the sidebands $b_{1,2}$, the expectation values for the efficiencies $\epsilon_{1,2}$, where the indices 1,2 refer to the leading and non-leading particles, respectively, and the expectation value for the combined signal s. The expectation values for the leading and non-leading signals were obtained for a given asymmetry A as: $s_{1,2} = s \cdot (1 \pm A) \cdot \epsilon_{1,2}$, where $\pm$ sign refer to the leading and non–leading particles, respectively. The likelihood function then was:

$$\mathcal{L}(A) = \prod_{i=1,2} \frac{e^{-(s_i+\alpha b_i)} \cdot (s_i + \alpha b_i)^{N_i}}{N_i!} \times \frac{e^{-b_i} \cdot b_i^{B_i}}{B_i!} \times e^{-((\epsilon_i - \mathcal{E}_i)/\sigma_i)^2/2}, \tag{2}$$

where the last term takes into account the statistical errors of the efficiency calculations. The likelihood function $\mathcal{L}(A)$ was maximised for each value of A with respect to the other parameters, taking into account the physical limits $s, b_{1,2} \geq 0$. The logarithms of the likelihood functions for the 1993 and 1994 data were added and the expectation value of asymmetry $\overline{A}$ was found at the maximum of the likelihood function $\mathcal{L}_{max}$. The 1σ confidence interval was found at the points of $ln(\mathcal{L}_{max}) - ln(\mathcal{L}) = 0.5$ within the allowed range $-1 \leq A \leq 1$. If only one such point existed a one-side error is given. Lower limits on the asymmetry at 90% confidence level, A_{min}, were obtained looking for a value $A < \overline{A}$ at $ln(\mathcal{L}_{max}) - ln(\mathcal{L}) = \Delta$, with Δ varying from Δ=0.82 for $\overline{A}$ being at least 2σ away from ± 1 to Δ=1.35 for $\overline{A}$=1.

The results are presented in Table 3 and in Fig. 4. Only the statistical errors are shown.

3.4 Systematic Errors

Systematic errors may come from charge asymmetries in the detection efficiencies, not accounted for in the simulation, or from beam contamination by particles different from Σ^-. The spectrometer acceptance does not impose any considerable charge asymmetry, though the acceptance of the RICH was slightly asymmetric. Possible effects of this asymmetry were studied comparing accepted and rejected events in different momentum ranges. Kaon identification criteria were not stringent. A typical efficiency of about 90% for such criteria was measured using clearly identifiable $\phi \rightarrow \mathrm{K^+K^-}$ decays. On the other hand, if stronger vertex cuts were used, relatively clean charm signals were seen even with very weak RICH cuts. It was observed that indeed the efficiency of the RICH cuts was not worse than 90%. A conservative estimate of the systematic error of A associated with the RICH efficiency is 3% over the full x_F range. Another possible source of systematic errors is the efficiency of the trigger, whose logic was charge dependent. In simulation the trigger caused an asymmetry of about 10% at high momenta. The trigger simulation has been compared with the data using a sample of minimum bias events recorded with minimal trigger requirements. Within these data a sample of Λ^0 decays was found, its trigger efficiency measured and compared to simulation of Λ^0 production. The simulated trigger efficiency was about 0.85 – 0.95 of the measured one. The difference can be attributed mainly to the multiplicity in the last scintillator hodoscope being higher in data than in simulation and is not charge dependent. A systematic error on A of 5% is assigned to account for uncertainties of the trigger efficiency.

Stability of the results on variations of the most important geometrical cuts was also studied. No statistically significant change of the measured asymmetries has been observed.

Another type of systematic error comes from beam contamination. The beam was identified by the TRD used in the trigger. During the data taking a sample of events with no beam interaction requirement was recorded. This sample was used to study the beam composition. Σ^- could be identified by their decays. The main contamination was π^- comprising 11% and 18% of the events used for the charm search for the 1993 and 1994 data respectively. This contamination could be reduced by an off-line analysis of the TRD information. Unfortunately, the full TRD information was available only for a part of the selected charm sample. This subsample was used to estimate the impact of the pion contamination. This impact depends on the type of the charmed particle studied. It was observed that the $D^{\pm}$ signal splits between the Σ^- and π^- beam subsamples proportionally to the beam composition, within the statistical accuracy, but no statistically significant D_s or Λ_c signal was observed in the pion beam subsample. $A(D^{\pm})$ measured in a π^- beam at 500 GeV/c [6] is shown in Fig. 4 as a curve fitted to these data. The results of our measurement indicate slightly higher asymmetries. If $A(D^{\pm})$ in both Σ^- and π^- beams were the same no systematic error would be added by a π^- contamination. In the extreme assumption that $A(D^{\pm})$ in a Σ^- beam were two times higher than in a π^- beam, the contamination may dilute the measured asymmetry by a factor of about 0.92. For the D_s and Λ_c, not more than 10% of the sample may originate from the pion component of the beam. Since no asymmetry for these particles has been observed in pion beams, a possible dilution factor in our measurement is not lower than 0.90. Another source of beam contamination comes from the decays of Σ^- in the beam to π^- and neutrons, when one of the decay products interacts in the charm production target. The pions cannot produce a competitive sample of charmed particles due to their low energy, but the neutrons can. In this data analysis no requirement of a beam track association with the reconstructed primary vertex was applied and therefore some part of the charm sample may be produced by neutrons. A number of neutron interactions at the 5% level was observed in the full sample of interactions recorded. Since neutrons contain two d-quarks, similar to Σ^-, one may expect similar asymmetries for $D^{\pm}$ and Λ_c produced by neutrons and Σ^- and therefore no dilution for $A(D^{\pm})$ and $A(\Lambda_c)$. If D_s^- production by neutrons were comparable with D_s^- production by Σ^- $A(D_s)$ could at most be diluted by a factor of about 0.95. The D_s^- signal is contaminated with not more than 8 D^- events. If $A(D_s)=A(D^{\pm})$ no systematic error would be added to $A(D_s)$ by this contamination. In the extreme assumption that $A(D_s)=2A(D^{\pm})$ the contamination may dilute the measured asymmetry by a factor of about 0.95. The contamination of the Λ_c signal with D^+ is below 3 events and its role is less significant.

For the estimate of the full systematic error of the asymmetry measurement we added in quadrature the errors coming from the efficiency uncertainties and obtained a value of about 6% over the full x_F range and for all the particles considered. Additionally, the values of the observed asymmetries may be diluted by a a factor of >0.9 due to the beam contamination. These systematic errors are smaller than the statistical errors of the measurement and therefore they are not considered in Table 3 and in Fig. 4.

4 Discussion

The asymmetry $A(D^{\pm})$ observed (Fig. 4) is similar to the results of pion beam measurements, though it is generally higher than the pion beam data by 1-2 standard deviations. The drop of the last point at $x_F=0.7$ is not statistically significant. The asymmetries $A(D_s)$ and $A(\Lambda_c)$ are generally higher than $A(D^{\pm})$.

The results have been compared with two theoretical calculations. In a parton model approach applied in [24] and earlier papers [25] PQCD is used to describe the charm quark production. The model considers two mechanisms contributing to the subsequent hadronisation. The first one is

fragmentation describing charm quark hadronisation in the absence of any interaction with quarks from initial hadrons. This process has been studied extensively in e^+e^- experiments and has been well described phenomenologically in terms of fragmentation functions. The second mechanism is recombination with valence quarks. A recombination function was constructed by analogy with the fragmentation functions and certain boundary conditions were applied to it. The resulting model depends on a few parameters included in the recombination function which were tuned to the charm production asymmetries measured in pion beams [24]. The main uncertainty comes from an unknown relative contribution of the recombination process. Using the same set of parameters predictions for the Σ^- beam were obtained [26]. The resulting predictions are shown in Fig. 4 and describe the data well.

Another theoretical calculation was performed applying the quark–gluon–string model (QGSM) to charm particle production [27–29] where charm particles are created in the break up of strings linked to valence quarks in the incoming hadron. In this approach a strong leading/non–leading production asymmetry at high x_F emerges from the momentum correlation of charm and valence quarks. This model was extended by adding a certain amount of charm sea similar to the one suggested in the "intrinsic charm" model [30]. The charm quarks and anti-quarks from the "charm sea" are assumed to have similar "hard" momentum distributions. In the string breaking process they are treated similarly to the valence quarks and the resulting production of charmed hadrons from the "charm sea" does not involve "normal" valence quarks of the colliding hadrons. Therefore the "charm sea" in this model contributes equally to the leading and non-leading particles at high momenta thus diluting the asymmetry [2]. The model contains two parameters one of which is the intrinsic charm amount, and should describe the production asymmetries and full charm cross–sections. The parameters have been tuned to the charm production asymmetries measured in pion beams. Using the same set of parameters predictions for $A(\mathrm{D}^\pm)$ and $A(\mathrm{D_s})$ in Σ^- beam were obtained [28]. These predictions are shown in Fig. 4 and also describe the data reasonably well.

5 Summary and conclusions

We have presented the first measurement of charge asymmetries of charmed particles produced in a Σ^- beam. Significant asymmetries in favour of leading over non–leading particles have been observed. The asymmetry observed for $\mathrm{D}^\pm$ production is compatible with the results obtained in pion beams. The results on $\mathrm{D_s}$ production point to a strong leading particle effect involving strangeness from the beam. And finally, a strong production asymmetry in favour of Λ_c baryon over $\overline{\Lambda}_\mathrm{c}$ anti-baryon is observed, in contrast with Λ_c production by pions. This confirms the indication of a strong leading particle effect with charmed baryons produced by baryon beams, reported by experiment E769 [12].

Acknowledgements

We are indebted to J. Zimmer and the late Z. Kenesei for their help during all moments of detector construction and set-up. We are grateful to the staff of CERN's EBS group for providing an excellent hyperon beam channel, to the staff of CERN's Omega group for their help in running

[2] It should be pointed out that the "intrinsic charm" model [30] led to a different result. This model considered recombination of the "intrinsic" charm quarks with valence quarks as an important process because of their close velocities. Therefore the valence quarks contribute to the momenta of the leading particles making them "harder" than the non–leading ones. The model predicted a considerable asymmetry $A(\mathrm{D}^\pm)$ at $x_F{>}0.5$ for π^- beams, however this prediction did not fit well to the data [6].

the Ω-spectrometer and also to the staff of the SPS for providing good beam conditions. We thank O. Piskounova and S. Slabospitsky for providing the predictions of their models for this experiment and G.H. Arakelyan and A.K. Likhoded for helpful discussions. The collaboration with O. Piskounova was supported by DFG (Germany) and RFBR (Russia) under contract number 436 RUS 113/332/2.

References

[1] WA89 Collaboration, M.I. Adamovich *et al.*, Z. Phys. **C76**, 35 (1997).

[2] P. Nason, S. Dawson and K. Ellis, Nucl. Phys. **B327**, 49 (1989).

[3] S. Frixione, M.L. Mangano, P. Nason, G. Ridolfi, Nucl. Phys. **B431**, 453 (1994).

[4] WA82 Collaboration, M.I. Adamovich *et al.*, Phys. Lett. **B305**, 402 (1993).

[5] E769 Collaboration, G.A. Alves *et al.*, Phys. Rev. Lett. **72**, 812 (1994).

[6] E791 Collaboration, E.M. Aitala *et al.*, Phys. Lett. **B371**, 157 (1996).

[7] BEATRICE Collaboration, M.I. Adamovich *et al.*, Nucl. Phys. **B495**, 3 (1997).

[8] ACCMOR Collaboration, S. Barlag *et al.*, Phys. Lett. **B247**, 113 (1990).

[9] E791 Collaboration, E.M. Aitala *et al.*, Phys. Lett. **B411**, 230 (1997).

[10] LEBC-EHS Collaboration, M. Aguilar-Benitez *et al.*, Z. Phys. **C40**, 321 (1988).

[11] ACCMOR Collaboration, S. Barlag *et al.*, Z. Phys. **C39**, 451 (1988).

[12] E769 Collaboration, G.A. Alves *et al.*, Phys. Rev. Lett. **77**, 2388 (1996).

[13] Yu.A. Alexandrov *et al.*, CERN-SL-97-60 EA, CERN, Geneva, Switzerland (1997)

[14] W. Brückner *et al.*, Nucl. Instrum. Methods **A378**, 451 (1996).

[15] W.Beusch, CERN–SPSC/77-70, CERN, Geneva, Switzerland (1977)

[16] W. Beusch *et al.*, Nucl. Instrum. Methods **A323**, 373 (1992); H.-W. Siebert *et al.*, Nucl. Instrum. Methods **A343**, 60 (1994); U. Müller *et al.*, Nucl. Instrum. Methods **A371**, 27 (1996).

[17] W. Brückner *et al.*, Nucl. Instrum. Methods **A313**, 345 (1992).

[18] C.V.Scheel, Dissertation,University Amsterdam, 1994.

[19] J.C. Lasalle *et al.*, Nucl. Instrum. Methods **A176**, 371 (1980).

[20] Review of Particle Physics, Particle Data Group, R.M. Barnett *et al.*, Phys. Rev. **D54** (1996).

[21] BEATRICE Collaboration, M.I. Adamovich *et al.*, Phys. Lett. **B385**, 487 (1996).

[22] H. Pi, Comput. Phys. Commun. **71**, 173 (1992)

[23] GEANT 3.21 CERN Program Library W5103, CERN 1993

[24] A.K. Likhoded and S.R. Slabospitsky, Phys. of Atomic Nuclei **60**, 981 (1997), translated from Yadernaya Fizika **60**, 1097 (1997); Preprint of IHEP 97–66, Protvino, 1997; hep-ph/9710476.

[25] V.G. Kartvelishvili, A.K. Likhoded and S.R. Slabospitsky, Yadernaya Fizika **33**, 832 (1981); A.K. Likhoded, S.R. Slabospitsky and M.V. Suslov, Yadernaya Fizika **38**, 727 (1983).

[26] S.R. Slabospitsky, private communications.

[27] O.I. Piskounova, Nucl. Phys. (Proc. Suppl.) **B50**, 179 (1996) and Phys. of Atomic Nuclei **60**, 439 (1997), translated from Yadernaya Fizika **60**, 513 (1997).

[28] O.I. Piskounova, private communications.

[29] G.H. Arakelyan and P.E. Volkovitsky, Z. Phys. **A353**, 87 (1995); G.H. Arakelyan, hep-ph/9711276 (1997).

[30] S.J. Brodsky, P. Hoyer, C. Peterson and N. Sakai, Phys. Lett. **B93**, 451 (1980); R. Vogt and S.J. Brodsky, Nucl. Phys. **B478**, 311 (1996).

Particle	Decay	# signal and background	Deviation from the PDG [20] mass MeV/c^2	Width MeV/c^2
D^-	$K^+\pi^-\pi^-$	296/38	0.3±1.5	8.5±0.5
D^+	$K^-\pi^+\pi^+$	142/42	-0.7±1.6	5.9±0.5
D_s^-	$K^+K^-\pi^-$	76/24	0.7±1.7	4.5±0.8
D_s^+	$K^+K^-\pi^+$	<27 90% CL		
Λ_c	$K^-p\pi^+$	74/20	1.9±1.7	5.0±0.6
$\overline{\Lambda}_c$	$K^+\overline{p}\pi^-$	<24 90% CL		

Table 1: Number of reconstructed signal events, background events and parameters of the mass fit.

x_F	D^-						D^+					
	run #1			run #2			run #1			run #2		
	N	B	$\mathcal{E}$ %	N	B	$\mathcal{E}$ %	N	B	$\mathcal{E}$ %	N	B	$\mathcal{E}$ %
0.1 - 0.2	23	17	3.1±0.1	51	29	5.1±0.2	15	11	3.3±0.1	26	25	4.9±0.2
0.2 - 0.3	44	36	8.4±0.3	62	36	12.1±0.3	28	37	8.8±0.3	40	34	12.6±0.3
0.3 - 0.4	31	19	12.3±0.4	41	41	17.6±0.4	27	23	12.8±0.4	19	28	18.1±0.4
0.4 - 0.5	20	24	14.4±0.6	28	19	21.8±0.6	8	26	14.7±0.6	7	21	20.2±0.6
0.5 - 0.6	8	5	14.5±0.7	13	7	21.1±0.8	0	7	15.5±0.7	5	13	20.2±0.7
0.6 - 0.7	5	3	10.4±0.9	2	3	14.5±1.0	4	6	11.5±0.9	2	11	16.3±1.0
0.7 - 0.8	2	1	7.4±0.9	2	1	14.3±1.1	1	0	9.8±1.0	0	3	14.5±1.1
	D_s^-						D_s^+					
0.1 - 0.2	5	17	2.2±0.1	8	35	3.6±0.1	6	17	2.5±0.1	6	24	3.2±0.1
0.2 - 0.3	13	19	6.5±0.2	25	19	9.5±0.2	13	30	6.9±0.2	4	23	9.9±0.2
0.3 - 0.4	7	12	9.4±0.3	15	27	13.5±0.3	4	21	10.7±0.3	3	12	14.4±0.3
0.4 - 0.5	6	9	12.0±0.5	10	8	15.5±0.4	3	9	12.7±0.6	0	10	17.8±0.4
0.5 - 0.6	2	5	11.6±0.8	5	5	16.6±0.6	1	2	12.3±0.9	2	5	17.4±0.6
0.6 - 0.7	4	0	8.4±1.3	0	1	15.4±0.7	1	2	11.8±1.5	2	2	16.6±0.8
	Λ_c						$\overline{\Lambda_c}$					
0.1 - 0.2	7	16	1.0±0.1	10	20	1.3±0.1	3	23	0.9±0.1	7	27	1.2±0.1
0.2 - 0.3	9	16	2.5±0.1	13	12	3.6±0.2	3	9	2.3±0.1	3	18	2.8±0.2
0.3 - 0.4	14	7	4.2±0.2	12	11	5.5±0.3	1	5	3.3±0.2	6	2	4.3±0.2
0.4 - 0.5	4	4	4.5±0.3	9	4	6.3±0.4	0	1	4.4±0.4	3	2	5.4±0.3
0.5 - 0.6	0	2	4.4±0.3	5	2	6.1±0.4	0	0	3.6±0.6	0	0	6.1±0.4
0.6 - 0.7	0	3	3.2±0.4	3	3	6.2±0.6	0	0	2.8±0.9	0	0	5.1±0.5

Table 2: The numbers of events observed in the signal mass band N, the number of background events observed in the side bands B and the calculated reconstruction efficiencies. The background expected in the signal band is about 16.7% of the observed one.

x_F	$D^\pm$		D_s		Λ_c	
	$\overline{A}$	A_{min}	$\overline{A}$	A_{min}	$\overline{A}$	A_{min}
0.1 - 0.2	$0.31^{+0.10}_{-0.11}$	0.17			$0.66^{+}_{-0.44}$	0.02
0.2 - 0.3	$0.27^{+0.09}_{-0.09}$	0.16	$0..73^{+0.21}_{-0.21}$	0.45	$0.79^{+}_{-0.29}$	0.37
0.3 - 0.4	$0.26^{+0.11}_{-0.11}$	0.12	$0.84^{+}_{-0.27}$	0.43	$0.49^{+0.17}_{-0.20}$	0.23
0.4 - 0.5	$0.70^{+0.15}_{-0.16}$	0.49	$1.00^{+}_{-0.14}$	0.66	$0.60^{+0.22}_{-0.27}$	0.24
0.5 - 0.6	$0.88^{+}_{-0.25}$	0.51	$0.51^{+0.39}_{-0.44}$	-0.08	$1.00^{+}_{-0.21}$	0.48
0.6 - 0.7			$0.79^{+}_{-0.40}$	0.10	$1.00^{+}_{-0.44}$	0.00
0.6 - 0.9	$0.27^{+0.34}_{-0.37}$	-0.20				

Table 3: The expectation values $\overline{A}$ and lower limits at 90% CL A_{min} for the asymmetries measured. Only the statistical errors are shown.

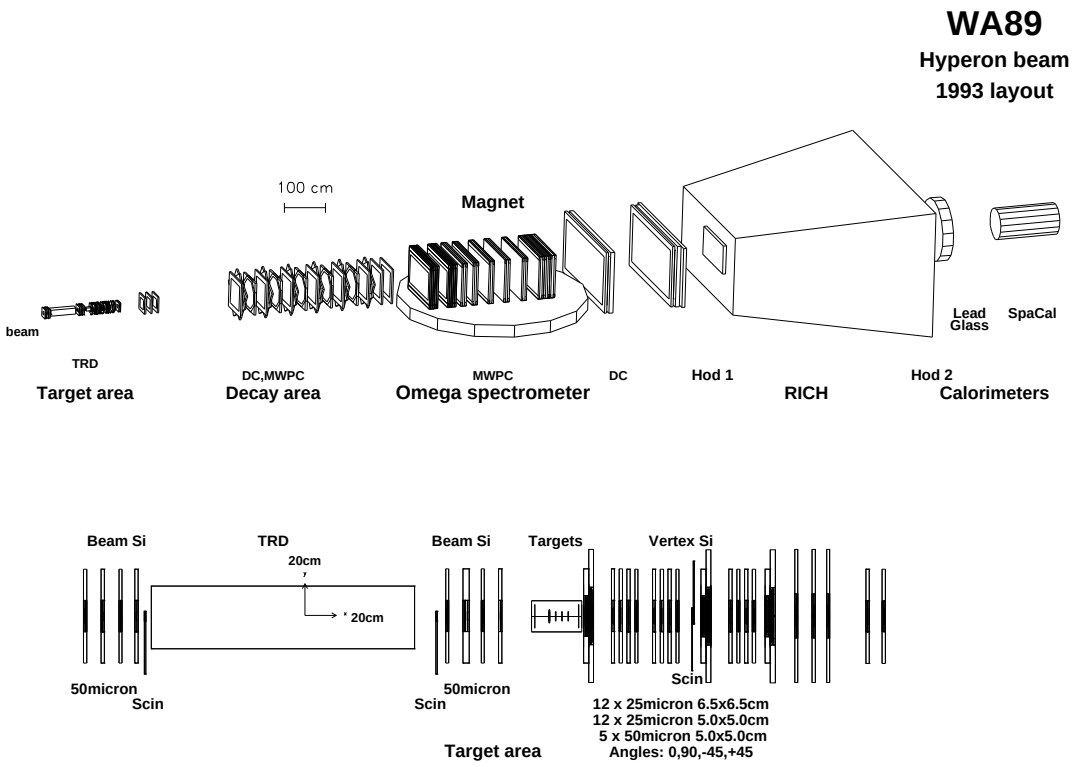

Figure 1: Setup of the WA89 experiment in the 1993 run. The lower part shows an expanded view of the target area.

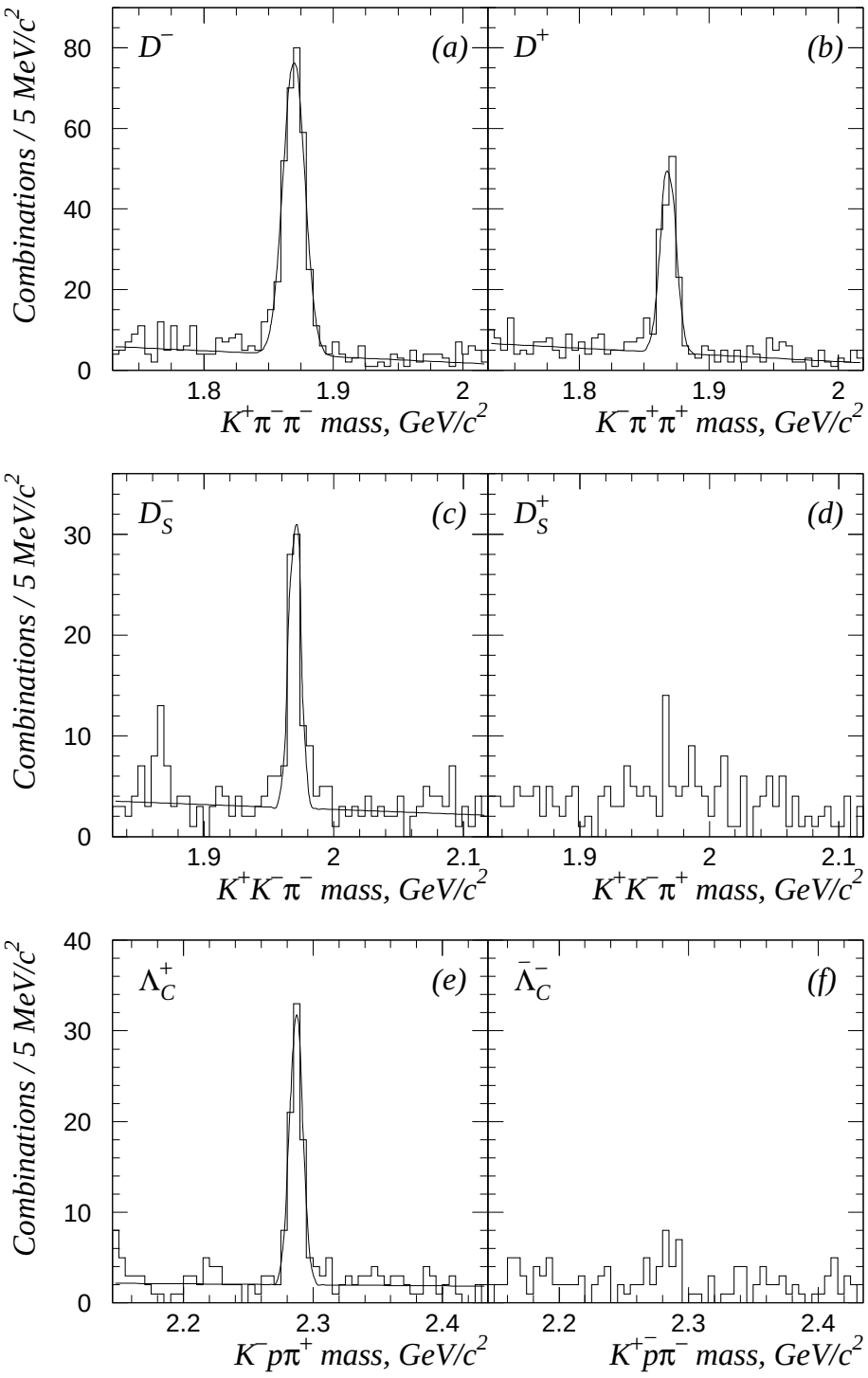

Figure 2: Invariant mass distributions for **(a)** $D^- \to K^+\pi^-\pi^-$, **(b)** $D^+ \to K^-\pi^+\pi^+$, **(c)** $D_s^- \to K^+K^-\pi^-$, **(d)** $D_s^+ \to K^-K^+\pi^+$, **(e)** $\Lambda_c \to K^-p\pi^+$, **(f)** $\overline{\Lambda}_c \to K^+\overline{p}\pi^-$.

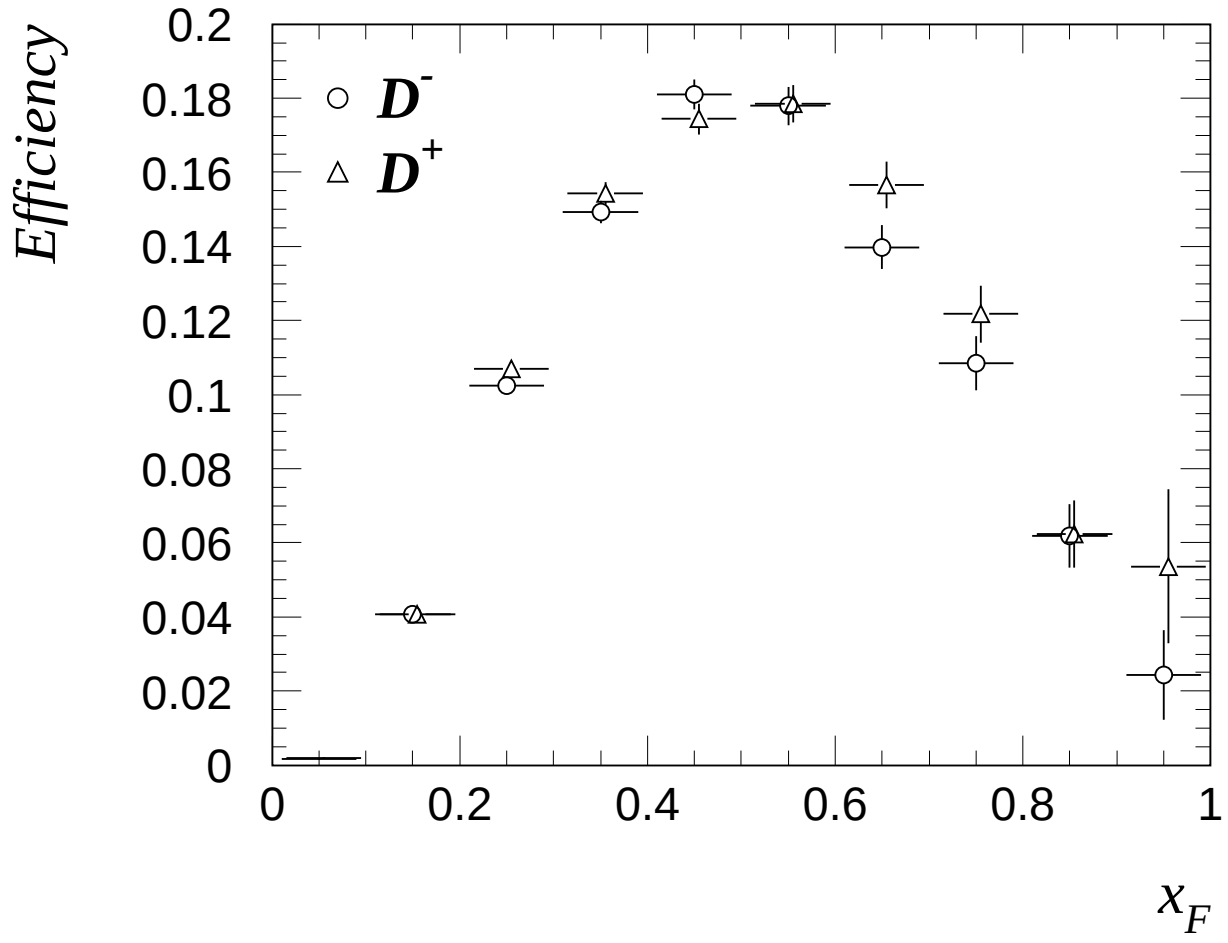

Figure 3: Full efficiency of $D^{\pm}$ meson reconstruction. The average values for the 1993 and 1994 runs of data taking are shown.

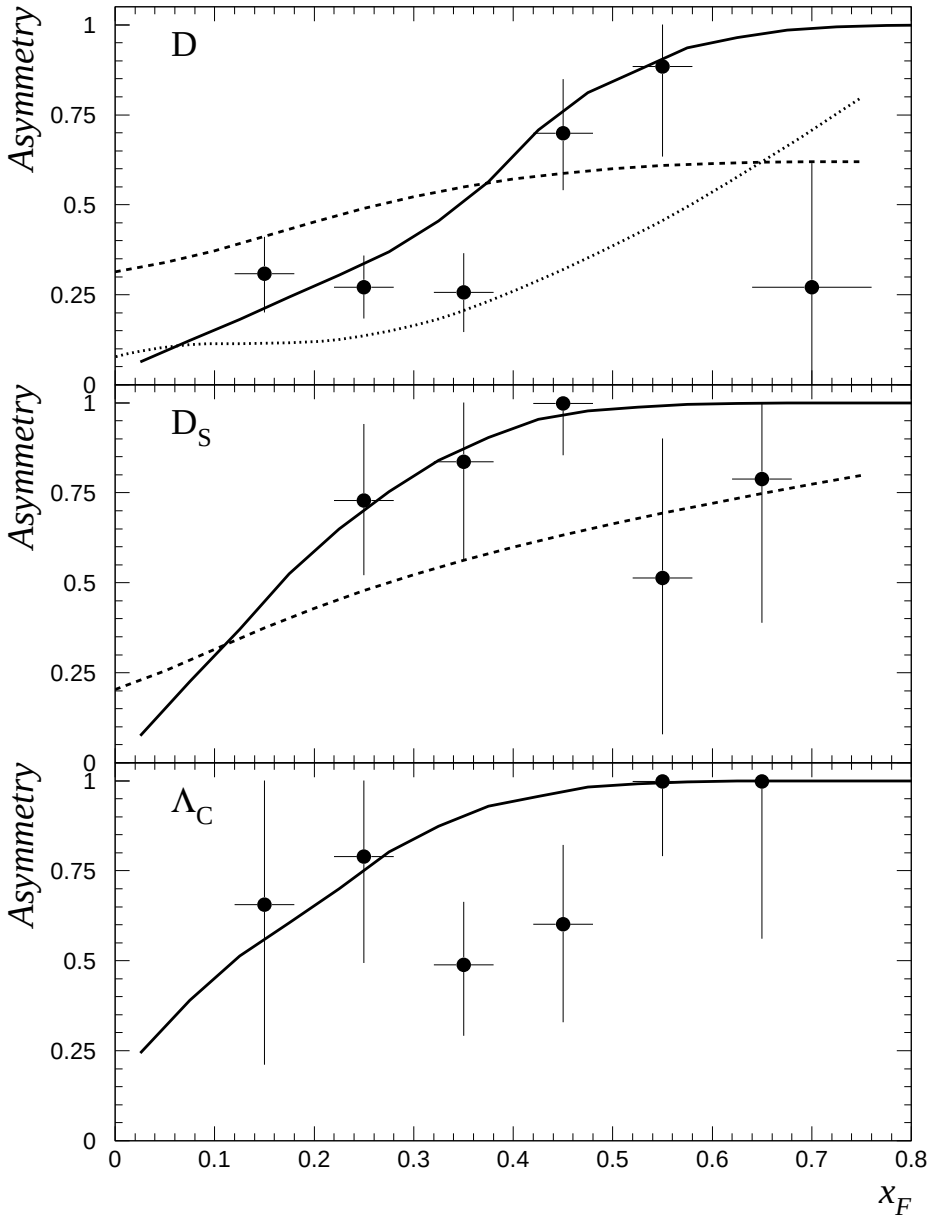

Figure 4: Asymmetries for $D^{\pm}$, D_s, and Λ_c production. The solid and dashed curves show the results of calculations [26] and [28], respectively. The dotted curve shows the tuned PYTHIA calculations for π^- beam taken from [6], which represent closely the results obtained by experiment E791 at FNAL.